NON-CONVENTIONAL ELECTRON MICROSCOPY IN SMALL DEFECT CHARACTERIZATION

Author
Seshan, K.

Publication Date
1974-02-01

Paper submitted to the Thirty-second Annual Meeting Electron Microscopy Society of America, St. Louis, MO, August 13-16, 1974.

LBL-2585 c.2

NON-CONVENTIONAL ELECTRON MICROSCOPY IN SMALL DEFECT CHARACTERIZATION

K. Seshan

February 1974

Prepared for the U. S. Atomic Energy Commission under Contract W-7405-ENG-48

DISCLAIMER

NON-CONVENTIONAL ELECTRON MICROSCOPY IN SMALL DEFECT CHARACTERIZATION

K. Seshan

Department of Materials Science and Engineering, University of California, Berkeley and Lawrence Berkeley Laboratory, Berkeley, California 94720.

The conventional bright field (Fig. 1a) and dark-field images of small (<200Å) defects are beset with several disadvantages: The image sizes (≈300Å) are two or three times the defect size; the image shift from core position may be larger than the defects; (Table 1a); the images are dominated by strain field effects and give no clue to defect shape and habit. Conventional images are therefore unsuitable for the size, nature and habit plane determination of small defects.

In this paper two recently announced non-conventional imaging techniques which yield narrow images (20-40Å) are applied to small defects. The same area is imaged in bright field in the symmetric weak-beam bright field (SWBBF) (1) and in the weak-beam (2) condition with two values of S_g in Fig. 1a,b,c,d respectively. See Table 1a,b for some characteristics of these images. The complexity of the bright field image makes measurements in column a unreliable.

TABLE 1

a. Image Characteristics b. Size Estimate of Loop B |g.b=1|

		a	b	c	d
a.	Figure 1	a	b	c	d
Image	Width Å	600	60	55	28
	Shift Å	210	±28	±28	calculated 20
	S_g	1.23×10^{-2}	5.36×10^{-3}	1.1×10^{-2}	1.61×10^{-2}
b.	Length Å	364	350	330	324
	Width Å	393	98	110	60
	Shift from Fig.1d. Å	115	20	25	0

Conclusions: This study demonstrates that non-conventional electron microscopy yields information on defect characteristics not available in conventional bright and dark field images. The weak-beam case (1d) shows one edge of loop A as a double line. Possibly loop A is perfect and has segments split into partial dislocations as was hypothesized for diamond shaped loops in aluminium (3). Hexagonal loops with fringes, e.g. loop C which is seen to intersect the foil surface, shows evidence of being steeply inclined to the foil surface.

These conclusions drawn from the weak-beam method show that whilst these images are difficult to obtain because of low visibility and long exposure times (64 sec), they are the most representative of loop size and shape.

The SWBBF (1b) is much easier to obtain than the weak-beam image and requires shorter exposure times (8 sec). It is still superior to the bright-field case although the image characteristics are more complicated. From Fig. 1b it is seen that some loops (loop C) show double images whereas others (B) show single images. As has been shown, this fact may be used to determine |g.b| from one image.

1. P.M. Kelly and R.G. Blake, Phil. Mag., 28, 475 (1973).
2. D.J.H. Cockayne, I.L.F. Ray and M.J. Whelan, Phil. Mag., 20, 1265 (1969).
3. A. Eikum, and G. Thomas, J.A.P., 34, No. 11, 3363 (1963).

Helpful discussions with Professor J. Washburn and Professor G. Thomas are gratefully acknowledged. The study was funded by the USAEC.

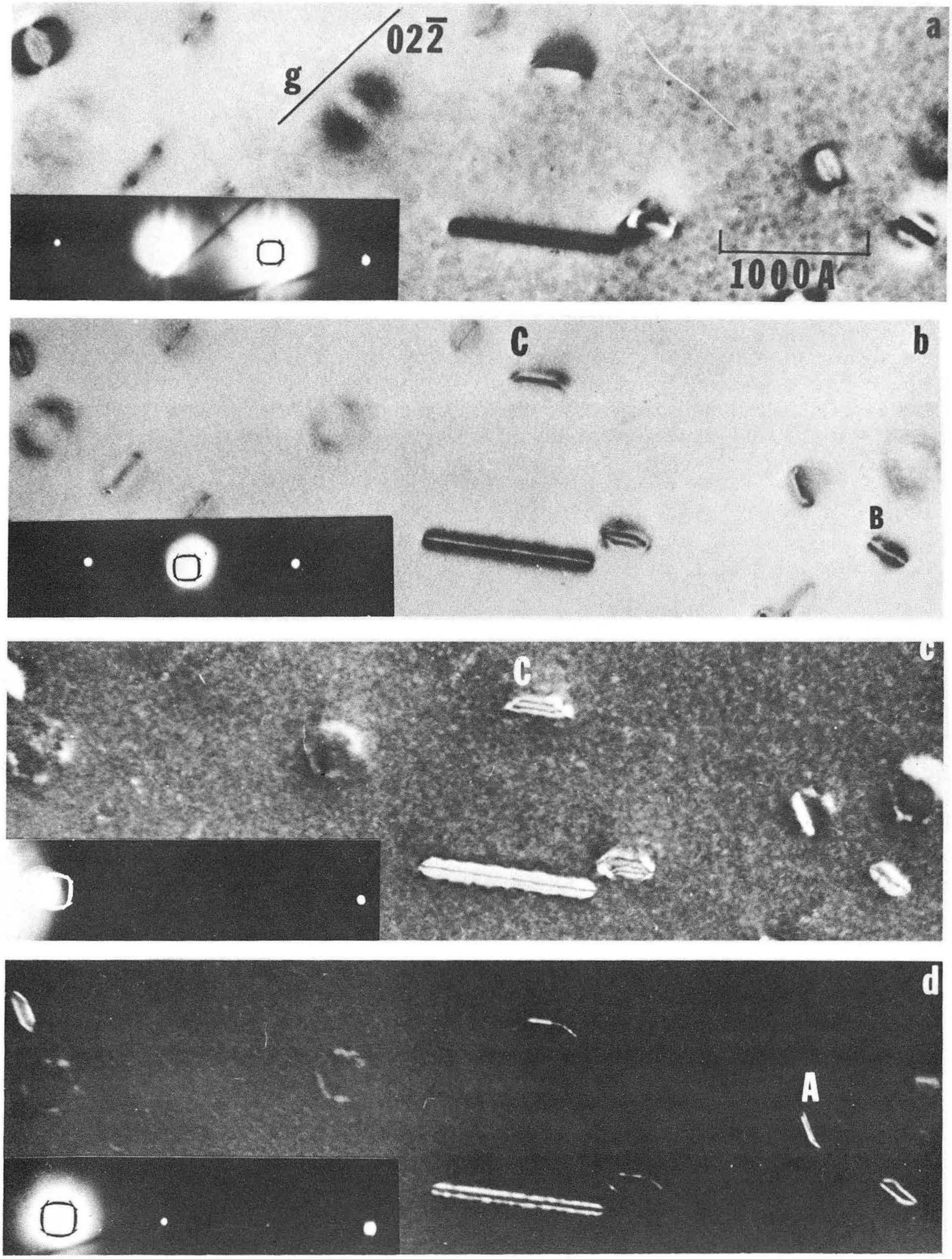

XBB 742-1268

Fig. 1
Shows the Fright-field (a) symmetric-weak-beam-bright-field SWBBF (b) and weak-beam images at Sg = 1.1×10^{-2}Å^{-1} (c) and at Sg = 1.61×10^{-2}Å^{-1} (d) of small defects in P^+ ion-implanted silicon.